Journal of Food Engineering 423 (2027) 113271

Contents lists available at ScienceDirect

Journal of Food Engineering

journal homepage: www.elsevier.com/locate/jfoodeng

Modelling the secondary shelf life of packaged breadsticks

Emanuela Lo Faro [a,b,1], Francesca Masino [a,b,1], Patrizia Fava [a,b], Matteo Alessandro Del Nobile [c,*], Amalia Conte [d]

[a] Department of Life Sciences, University of Modena and Reggio Emilia, Via G. Amendola 2, Reggio Emilia, 42122, Italy
[b] Interdepartmental Centre BIOGEST-SITEIA, p.le Europa 1a, Reggio Emilia, 42124, Italy
[c] Department of Economics, Management and Territory, University of Foggia, via A. da Zara 11, Foggia, 71122, Italy
[d] Department of Humanities. Letters, Cultural Heritage and Educational Studies, University of Foggia, via Arpi 176, Foggia, 71121, Italy

ARTICLE INFO

Keywords:
Breadstick
Shelf life
Secondary shelf life
Modelling

ABSTRACT

The aim of this study was to establish a correlation between the secondary shelf life (SSL) of packaged breadsticks and their residual shelf life (RSL). To this aim, the packaged product was stored at 38 °C and external water activity of 0.912. Throughout the entire storage period, the internal water activity was monitored. At regular time intervals (every 7 days), the primary package was opened, and the internal water activity continued to be monitored. The above set of data were used to estimate both the primary shelf life (PSL) and the SSL. To this aim, two different models were proposed to describe the experimental data. The first assumes, among the other hypotheses, that the water sorption isotherm can be described by the GAB model, whereas the second assumes a linear relationship between the water absorbed by the breadsticks and the water activity. Both mathematical approaches were found satisfactory. Accordingly, the PSL and SSL values obtained from the two models were very similar. Considering the complexity of the models and their performance in describing the data, the approach based on a linear water sorption isotherm appears the most appropriate, as it offers a good balance between accuracy and simplicity. As expected, SSL is consistently lower than RSL and decreases as RSL decreases.

1. Introduction

Household food waste often increases after a product has been opened, largely due to uncertainty regarding its actual remaining shelf life. While packaging typically reports a “best before” or expiration date referring to unopened items, it rarely provides clear information on how long the food remains acceptable once the package has been opened (Panel et al., 2020). As a result, consumers frequently discard food prematurely out of precaution, even when it may still be suitable for consumption. According to the Waste and Resource Action Programme (Wrap, 2023), approximately 41% of household food waste consists of still-edible food. It is estimated that a proper information campaign, combined with clear labelling, could reduce waste by approximately 350,000 tons per year, with significant economic and environmental benefits, considering that food waste accounts for between 8% and 10% of greenhouse gas emissions (Chen and Chau, 2026). Therefore, improving the scientific basis for post-opening shelf-life estimation represents an important step towards more sustainable food consumption (Martinelli et al., 2025).

From a scientific perspective, this issue requires distinguishing between primary shelf life (PSL) and secondary shelf life (SSL). Primary shelf life is defined as the period between packaging and the time when the product is no longer acceptable under the recommended storage conditions. It depends on product characteristics, processing conditions, packaging properties and storage environment. Once these conditions are altered, for example by opening the package or changing storage temperature, deterioration mechanisms generally accelerate (Zardetto et al., 2022). The period between this modification and product rejection is referred to as secondary shelf life (SSL) (Nicoli and Calligaris, 2018). Although both concepts describe product durability, modelling PSL and SSL poses fundamentally different challenges. PSL prediction aims at estimating a single value corresponding to the end of product acceptability (Tsironi et al., 2009). Conversely, SSL cannot be represented by a unique value because it depends on the moment at which the

* Corresponding author.
E-mail addresses: emanuela.lofaro@unimore.it (E. Lo Faro), francesca.masino@unimore.it (F. Masino), patrizia.fava@unimore.it (P. Fava), matteo.delnobile@unifg.it (M.A. Del Nobile), amalia.conte@unifg.it (A. Conte).
[1] These Authors contributed equally to this work.

https://doi.org/10.1016/j.jfoodeng.2026.113271
Received 12 May 2026; Received in revised form 29 June 2026; Accepted 30 July 2026
Available online 3 August 2026

primary storage conditions are interrupted. Therefore, SSL should be regarded as a dynamic function of the product state at opening rather than as a fixed characteristic. Developing predictive approaches for SSL thus requires not only modelling the deterioration mechanisms occurring after opening but also quantifying how the product degradation accumulated during the primary shelf life affects the residual stability after package opening.

Extensive literature is available on predictive modelling of PSL (Cui et al., 2023; Coffigniez et al., 2021; Piergiovanni and Limbo, 2019), whereas predictive approaches specifically addressing SSL remain scarce (Li et al., 2024). Recently, increasing attention has also been devoted to predictive approaches capable of describing food quality evolution under realistic storage conditions, where multiple environmental variables simultaneously affect product deterioration. In this context, statistical tools such as Response Surface Methodology have been employed to evaluate the combined effects of different process or storage factors (Salimbahrami et al., 2023), while data-driven approaches based on Grey System Theory have proved particularly suitable for modelling shelf-life evolution from limited or incomplete experimental datasets, as typically encountered in *in vivo* studies (Afsharnia, 2023).

Regarding SSL, Del Nobile and Conte (2023), reviewing studies published between 2001 and 2022, identified only sixteen papers dealing with SSL of shelf-stable foods. Their review introduced the concept of residual shelf life (RSL), defined as the time required for a packaged product, stored under its original conditions, to reach the acceptability limit at any given storage time. RSL therefore ranges from the entire PSL at packaging (t = 0) to zero when the product reaches the end of its primary shelf life (Del Nobile and Conte, 2023). Among the studies reviewed, only Cesa et al. (2015) and Nicosia et al. (2022) explicitly investigated the dependence of SSL on RSL, demonstrating that the remaining post-opening shelf life varies according to the time at which the package is opened. More recent studies have mainly focused on specific factors affecting SSL, including the use of natural preservatives (Sordini et al., 2024, 2025), the residual effect of modified atmosphere packaging gases (Bianchi et al., 2024), closure systems for wine bottles (Bianchi et al., 2023), and the influence of environmental conditions on powdered infant milk through Arrhenius-based models (Li et al., 2024; Jia et al., 2025).

Although these methodologies provide valuable tools for predicting food quality under variable conditions, they mainly focus on estimating product shelf life under specific storage scenarios and do not explicitly address the quantitative relationship between residual shelf life and secondary shelf life after package opening. No general mathematical framework is currently available to quantitatively relate SSL to RSL for moisture-sensitive foods packaged in permeable materials. Therefore, the novelty of the present work lies in the development of a predictive mathematical framework capable of establishing a quantitative relationship between residual shelf life and secondary shelf life for moisture-sensitive dry foods packaged in permeable polymeric materials. Rather than estimating SSL only under specific experimental conditions, the proposed approach aims to describe how post-opening shelf life evolves as a function of the degradation accumulated before opening, thus providing a general modelling framework potentially applicable to different products sharing similar deterioration mechanisms. To validate the proposed methodology, breadsticks packaged in single-serving polypropylene bags grouped within an external polypropylene multipack were selected as a representative model system for moisture-sensitive dry foods. Under intact packaging conditions, PSL is governed by the combined barrier properties of the two packaging layers. After removal of the external package, the individual units become directly exposed to the surrounding atmosphere, accelerating moisture transfer and quality degradation. Samples were stored in a climatic chamber and, at predefined intervals, the external package was removed while water activity evolution was monitored. Sensory evaluation was performed to identify the critical moisture level corresponding to product rejection by 25% of assessors. These experimental data were used to estimate PSL, RSL and SSL and to validate the proposed mathematical relationship between residual and secondary shelf life.

2. Materials and methods

2.1. Materials

The samples investigated in this study consisted of *mini*-format breadsticks supplied by an Italian manufacturer. The breadsticks were approximately 55 mm in length, with a mean diameter of 8 mm and were characterized by the presence of coarse sodium chloride crystals on the surface. They were packaged in single-serving pouches, and 8 individual pouches were grouped into an external multipack. The weight of the breadstick single pack was determined using an analytical balance (Sartorius AX224, Göttingen, Germany; capacity 220 g, resolution 0.1 mg, repeatability ± 0.2 mg). Each individual inner package contained 21.44 ± 0.277 g of breadsticks. Measurements were performed in 20 replicates to calculate the mean and standard deviation. A total of 36 multipacks were analyzed according to the Design of Experiments (DOE) detailed in the following section. In Fig. 1, a schematic representation of the packaging configuration is shown. The external flexible film is represented by a green rectangle with a red outline, while the individual pouches are depicted as yellow rectangles with black outlines and the breadsticks as grey spheres.

2.2. Packaging characterization

The outer packaging material was a multilayer structure composed of a 20-μm oriented polypropylene (OPP) layer (density equal to 0.91 $\frac{g}{cm^3}$), a 35-μm OPP COEX Pearl layer, (density equal to 0.74 $\frac{g}{cm^3}$) and the corresponding adhesive layer used for lamination (Sititalia S.p.A., San Marino, Italy). The inner packaging film was also a multilayer laminate, consisting of two 15-μm OPP COEX layers (density equal to 0.91 $\frac{g}{cm^3}$) bonded together by an adhesive layer (Sititalia S.p.A., San Marino, Italy). The outer film exhibited a Water Vapor Transmission Rate (WVTR) of 2.018 ± 0.112 $\frac{gH_2O}{m^2 \cdot 24\ h}$, a thickness of 60.00 ± 1.721 μm. The corresponding values for the inner film were 3.038 ± 0.156 $\frac{gH_2O}{m^2 \cdot 24\ h}$, 43.93 ± 6.212 μm, and 221.956 ± 2.2, respectively. The WVTR was measured according to the ASTM E96/E96M-24a (ASTM, 2024) standard method, with slight modification as described by (Lo Faro et al., 2021). For a detailed description of the procedure, the reader is referred to the original publication. Briefly, 25 mL glass vials were filled with 10 g of silica gel to create an internal relative humidity (RH) of 0%. The samples were securely attached to the vial openings, with the coated side facing inward to prevent tangential water vapor diffusion and incubated in a climate chamber (CH 150—CLIMATEST, ARGO LAB, Giorgio Bormac, Carpi, MO) set at 38 ± 1 °C and 90% RH. Vial weights were recorded twice daily throughout the 5-day test period. The WVTR value was calculated using the following formula:

$$WVTR = \frac{\Delta W}{\Delta t \cdot A} \cdot 24$$

where $\frac{\Delta W}{\Delta t}$ represents the slope of the linear regression of the mass gain versus time expressed as $\frac{gH_2O}{h}$, and A corresponds to the exposed surface of the film ($7.85 \cdot 10^{-5}$ m^2). Mean values and standard deviations were calculated from five independent replicates.

Thickness measurements for the inner and outer packaging films were conducted using a digital micrometer with a resolution of 0.001 mm (Syntek, New York, NY, USA). All evaluations were performed in a controlled environment maintained at 25 °C and 45% relative humidity (RH). Mean values and standard deviations were calculated from ten independent replicates. For both the inner and outer packages, the total surface area and the effective area available for mass

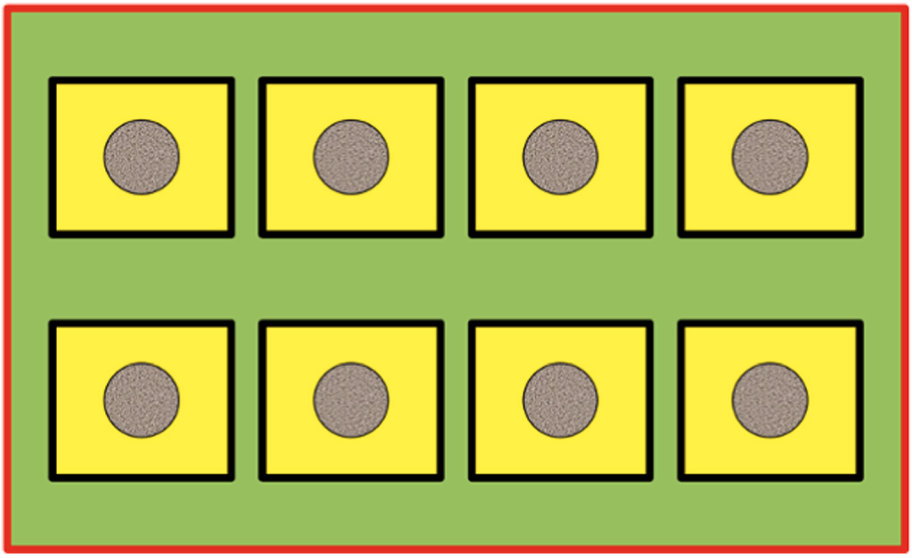

Fig. 1. Schematic representation of the primary and secondary packaging of breadsticks.

transfer were experimentally measured. The dimensions (length, *L*, and width, *W*) of the empty, flattened pouches were measured using a digital micrometer with a resolution of 0.001 mm (Syntek, New York, NY, USA). The total surface area was calculated according to the equation $Area = 2 \cdot (L \cdot W)$, thereby including both sides of the packaging. For the outer package the total surface area is $1582.2 \pm 12.66\ cm^2$; whereas the effective area available for mass transfer is $1362.4 \pm 14.24\ cm^2$. For the inner package the total surface area is $276.5 \pm 2.3\ cm^2$; whereas the effective area available for mass transfer is $221.9 \pm 2.2\ cm^2$. Mean values and standard deviations were calculated from ten independent replicates.

2.3. Design of experiment (DOE)

The experimental design was based on an Accelerated Shelf-Life Testing (ASLT) protocol aimed at simultaneously evaluating the

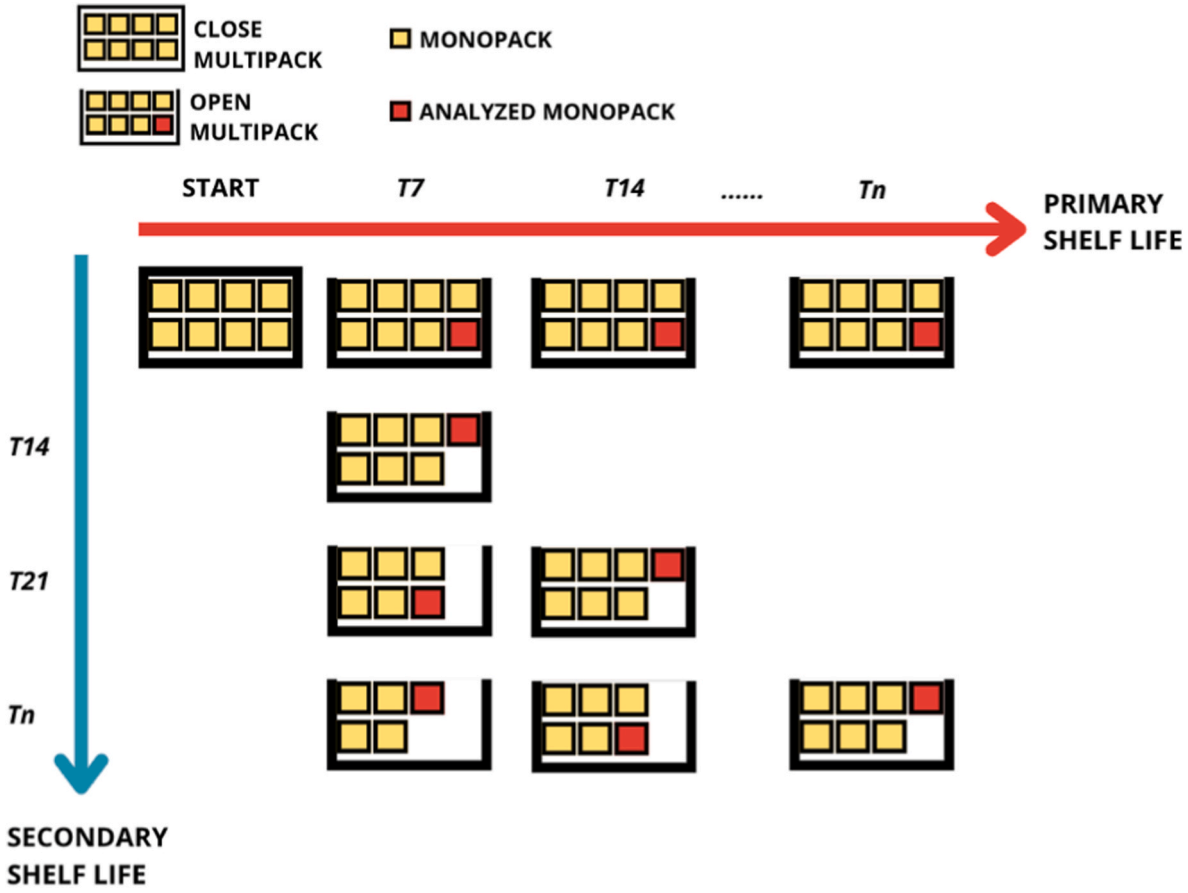

Fig. 2. Schematic representation of the experimental plan.

Primary Shelf Life (PSL) of intact packages and the Secondary Shelf Life (SSL) following package opening. Samples were stored in a climatic chamber (ARGOLab CH 150 CLIMATEST, Carpi, Modena, Italy) under accelerated conditions (38 ± 0.5 °C and 90 ± 2% RH). Temperature and relative humidity within the chamber were continuously monitored using mini dataloggers (Verigo PA2, Verigo, Sunnyvale, CA, USA) distributed throughout the storage area. Sampling was performed at weekly intervals (T_0, T_7, T_{14} … T_n), involving one mono-pack from four independent multipacks ($n=4$) at each time point. For PSL determination, one mono-pack was analyzed immediately after the opening of each multipack (T_x). Concurrently, SSL was assessed using a matrix-based experimental design: following the initial opening of the multipacks at time T_x, the remaining single-serving units were maintained under the same storage conditions and analyzed at subsequent intervals (T_{x+7}, T_{x+14} … T_{x+Tn}). The approach is illustrated in Fig. 2.

2.4. Water activity of breadsticks

Water activity (a_w) was measured at a controlled temperature of 25 °C using a dew point hygrometer (AquaLab Series 4 TE, Decagon Devices, Inc., Pullman, WA, USA). Before each analytical session, the instrument was calibrated using standard salt solutions of known a_w values. All determinations were performed in quadruplicate, and results are reported as mean ± standard deviation.

2.5. Sensory assessment of the critical water concentration

Sensory analysis was carried out exclusively on breadstick samples obtained from the PSL protocol by a panel of eight trained assessors (males and females, aged 20–60 years), selected in accordance with UNI EN ISO 8586:2023 requirements. Evaluations were performed in a sensory laboratory equipped with individual sensory booths under controlled environmental conditions (21 ± 1 °C and 50 ± 5% RH) and standardized daylight-type illumination, following the UNI ISO 8589:2014 and UNI EN ISO 13299:2016 standards. Before the sensory evaluation, the assessors underwent a specific training session aimed at establishing a common descriptive vocabulary and defining reference standards for the sensory attributes considered, namely friability, crispness, hardness, and rancidity. Panel performance was subsequently verified through ranking tests to assess the assessors' discriminative ability. During the Quantitative Descriptive Analysis (QDA) sessions, samples were served in a balanced order and coded for blind evaluation; assessors rated attribute intensity on a 10 cm structured linear scale (1: minimum intensity; 10: maximum intensity). Palate-cleansing intervals (water and apple) were provided between samples to prevent sensory fatigue. Each sensory session included the duplicate evaluation of two samples: freshly produced breadsticks used as the reference and breadsticks stored for the corresponding primary shelf-life time point. Finally, overall acceptability was determined via a binary test, setting the end of the experimental period when the acceptability threshold fell below 75%. The sensory analysis was conducted to determine the critical water concentration, defined as the threshold above which the breadsticks were considered unacceptable by consumers.

2.6. Determination of water sorption isotherm

Sorption isotherms were determined to define the equilibrium relationship between water concentration (c_w) and water activity (a_w) of the breadsticks, providing the necessary dataset for the validation of the proposed theoretical model. The experimental procedure was conducted following the static gravimetric method at a controlled temperature of 38 ± 0.5 °C (Calligaris et al., 2008; Lee and Robertson, 2021; Türksever et al., 2025). To characterize the full hygroscopic spectrum of the product, an a_w range between 0.11 and 0.90 was investigated. These conditions were generated within hermetically sealed chambers using saturated salt solutions and aqueous glycerol solutions at calibrated concentrations (Table 1).

For each experimental condition, the samples were analyzed in duplicate. Before storage, each sample was weighed using an analytical balance (Sartorius AX224, Göttingen, Germany; capacity 220 g, resolution 0.1 mg, repeatability ± 0.2 mg) and then placed on dedicated supports inside the microenvironments. The achievement of thermodynamic equilibrium between the product matrix and the surrounding atmosphere was monitored through periodic weighing at 48, 72, and 144 h. The equilibrium was assumed when the variation in mass between two consecutive weighing measurements was less than 0.1%.

2.7. Statistical analysis

Data of fitting parameters were compared using the one-way analysis of variance (ANOVA). HSD of Tukey, with the option of homogeneous groups ($p < 0.05$), was carried out to determine significant differences among samples. To the aim, JMP 18 for Windows (JMP Statistical Discovery LLC 920 SAS Campus Drive, Cary, NC 27513, USA) was adopted.

3. Results and discussion

As previously stated, the objective of this study was to establish the relationship between SSL and RSL. To this aim, two mathematical models describing the evolution of the internal water activity were developed based on the main mechanisms responsible for breadstick deterioration during storage. Following model validation, the predicted shelf-life values were used to establish the correlation between SSL and RSL.

3.1. Critical water concentration

The quality deterioration of breadsticks and similar low-moisture baked goods is mainly governed by two degradation mechanisms: moisture uptake, which progressively reduces friability and crispness, and lipid oxidation, which promotes the formation of off-flavours associated with rancidity. Although these processes generally occur simultaneously, their relative contribution to quality loss depends on storage conditions and the barrier properties of the packaging system. Recent research has extensively focused on strategies to mitigate lipid oxidation (Mora et al., 2025). For instance, Bianchi et al. (2021) evaluated the oxidative stability of experimental breadsticks enriched with natural antioxidants, such as grape pomace powder, using the OXITEST method. Similarly, Giuffrè et al. (2023) explored the incorporation of phenolic-rich extracts from olive leaves and olive mill wastewater into gluten-free formulations as a mean of extending shelf-life. Other studies have investigated synergistic effects, such as the combined use of rosemary extract and modified atmosphere packaging (100% N_2) to reduce oxidation rates (Alamprese et al., 2017). A common limitation among these studies is that storage was typically conducted under ambient conditions, with temperatures ranging from 15 to 25 °C, while relative humidity (RH) was either uncontrolled or remained low. In other studies, temperature was considered the sole accelerating factor, while

Table 1
List of saturated solution and solute used for water vapor sorption isotherm of breadsticks.

Lithium Chloride (LiCl)	0.11	Saturated solution (85 g/100 mL H_2O)
Potassium Acetate (CH_3COOK)	0.23	Saturated solution (255 g/100 mL H_2O)
Magnesium Chloride ($MgCl_2$)	0.33	Saturated solution (80 g/100 mL H_2O)
Glycerol	0.40	84.7% (w/w) aqueous solution
Glycerol	0.50	78.7% (w/w) aqueous solution
Glycerol	0.60	70.9% (w/w) aqueous solution
Glycerol	0.70	61.0% (w/w) aqueous solution
Sodium Chloride (NaCl)	0.75	Saturated solution (38 g/100 mL H_2O)
Glycerol	0.80	48.1% (w/w) aqueous solution
Glycerol	0.90	31.7% (w/w) aqueous solution

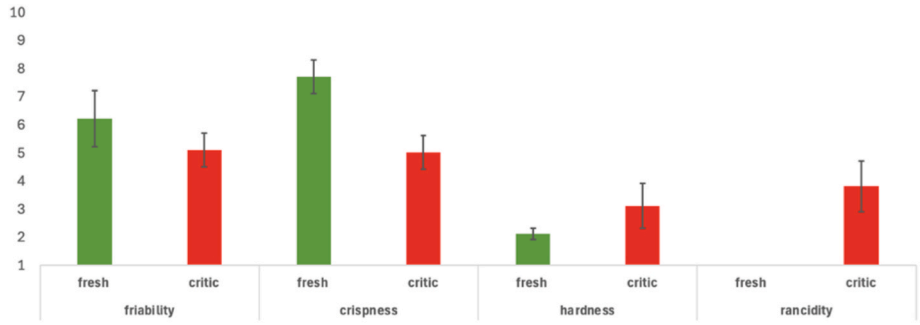

Fig. 3. Fresh *vs* unacceptable breadsticks (under 75%).

the effect of hygroscopic stress was not taken into account. In the present work, both storage temperature (38 °C) and relative humidity (90%) were employed as extrinsic factors to accelerate product decay. Consequently, the sensory panel was specifically trained to evaluate both textural degradation and rancidity. Fig. 3 illustrates the sensory profile of the fresh breadsticks, highlighting the specific attributes identified by the assessors as critical indicators of quality loss. Overall acceptability progressively declined with increasing moisture content, mainly as a consequence of textural deterioration. In particular, the reduction in friability and crispness occurred during the early stages of storage, whereas hardness and rancidity became appreciable only at more advanced stages (data not shown). This behavior is consistent with the kinetics of lipid oxidation in low-moisture foods. Previous studies have shown that increasing moisture content may enhance the oxidative stability of lipid-containing foods by promoting a temporal separation between the formation of primary oxidation products (hydroperoxides) and the subsequent generation of secondary volatile compounds, such as aldehydes, which are responsible for rancid off-flavors. Although the relationship between moisture content and lipid oxidation is complex and still not fully understood (Mora et al., 2025), a detailed investigation of these mechanisms is beyond the scope of the present study. Starting from this consideration and the data obtained, the overall acceptability of the samples showed a sharp decline upon reaching the water concentration threshold (c_w^{max}) that was found equal to 0.0915 $\frac{g\ H_2O}{g\ dm}$. Beyond this threshold value, the product was considered unacceptable due to loss of its characteristic sensory texture profile.

3.2. Modelling

In this section are presented the models used to describe the main phenomena responsible for the deterioration of packaged breadsticks, along with the assumptions adopted for their derivation.

3.2.1. Water sorption isotherm

The Guggenheim-Anderson-de Boer (GAB) model was used in this work to describe the water sorption isotherm of the investigated breadstick (Barbosa-Cánovas et al., 2007):

$$c_w = \frac{m_0 \cdot k \cdot C \cdot a_w}{(1 - k \cdot a_w) \cdot (1 - k \cdot a_w + C \cdot k \cdot a_w)} \tag{1}$$

where: c_w is the breadstick water concentration expressed as $\frac{g\ H_2O}{g\ dm}$, m_0 is the monolayer moisture content expressed as $\frac{g\ H_2O}{g\ dm}$, k and C are model constants related to the energetic interactions between water molecules and the absorbing media, and a_w is the water activity.

The kinetics of water absorption in dry products such as breadsticks has often been described using the GAB model (Collazos-Escobar et al., 2023; McMinn et al., 2007). More than one reason justifies the GAB adoption among the various models available in the literature. GAB provides a physically meaningful framework that captures multilayer sorption phenomena, distinguishes between strongly bound monolayer water and more weakly associated layers, and reliably fits experimental isotherms across a wide range of water activities, temperatures, and compositions, thereby enabling consistent comparison among products (Al-Muhtaseb et al., 2002).

3.2.2. Primary shelf life

The equation derived from the water mass balance in the volume between the outer film and the internal pouch is reported below:

$$\frac{dm_w^m(t)}{dt} = A^{est} \cdot \left[\frac{P_w^{est}}{\ell^{est}} \cdot \left(p_w^{est} - p_w^m(t)\right)\right] - A^{int} \cdot \left[\frac{P_w^{int}}{\ell^{int}} \cdot \left(p_w^m(t) - p_w^{int}(t)\right)\right] \tag{2}$$

where: $m_w^m(t)$ is the mass of water in the volume between the outer film and the internal pouch, t is the time, A^{est} is the exchange area of the outer film, P_w^{est} is the water permeability of the outer film, ℓ^{est} is the thickness of the outer film, and p_w^{est} is the water vapor partial pressure outside the primary package, $p_w^m(t)$ is the water vapor partial pressure in the volume between the outer film and the internal pouch, A^{int} is the exchange area of the internal pouch, P_w^{int} is the water permeability of the internal pouch, ℓ^{int} is the thickness of the internal pouch, and $p_w^{int}(t)$ is the water vapor partial pressure inside the internal pouch.

The equation derived from the water mass balance inside the internal pouch is reported below:

$$\frac{dm_w^{int}(t)}{dt} = A^{int} \cdot \left[\frac{P_w^{int}}{\ell^{int}} \cdot \left(p_w^m(t) - p_w^{int}(t)\right)\right] \tag{3}$$

where: $m_w^{int}(t)$ is the mass of water in all the internal pouches.

If it is assumed that the rate of water vapor accumulation in the volume between the outer and internal pouches (i.e., $\frac{dm_w^m(t)}{dt}$) is negligible, it can be shown that the following relation holds:

$$\frac{dm_w^{int}(t)}{dt} = \xi \cdot \left(p_w^{est} - p_w^{int}(t)\right) \tag{4}$$

where: $\xi = \frac{A^{int} \frac{P_w^{int}}{\ell^{int}}}{1 + \frac{A^{int} \frac{P_w^{int}}{\ell^{int}}}{A^{est} \frac{P_w^{est}}{\ell^{est}}}}$.

It is worth noting that $m_w^{int}(t)$ is the sum of two contributions:

$$m_w^{int}(t) = m_w^{ab}(t) + m_w^{hs}(t) \tag{5}$$

where: $m_w^{ab}(t)$ is the mass of water absorbed by the packaged food and $m_w^{hs}(t)$ is the mass of water in the headspace of each internal pouch.

If it is assumed that: *(i)* water vapor behaves as an ideal gas, *(ii)* water vapor in the headspace of the internal pouch is constantly in equilibrium with the water absorbed by the packaged breadsticks, *(iii)* water absorbed can be described by the GAB model (Equation (1)), it can be shown that the following relation holds:

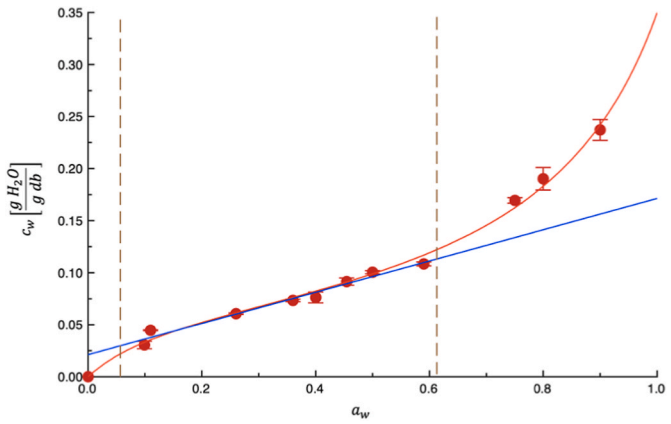

Fig. 4. Water sorption isotherm data (●), ——— best fit of Equation (1), ——— linear best fit of data within the range delimited by the two dashed vertical lines.

$$\frac{da_w^{int}(t)}{dt} = \frac{\xi \cdot p_w^0 \cdot \left(a_w^e - a_w^{int}(t)\right)}{M_w \cdot \frac{p_w^0 \cdot V_{hs}}{R \cdot T} + m_{ss} \cdot \frac{m_0 \cdot k \cdot C \cdot \left(y_2 \cdot y_3\right) - y_1 \cdot \left[-k \cdot y_3 + y_2 \cdot (C \cdot k - k)\right]}{\left(y_2 \cdot y_3\right)^2}} \tag{6}$$

where: $a_w^{int}(t)$ is the water vapor activity in the internal pouch headspace, p_w^0 is water vapor pressure, M_w is the water molecular weight, V_{hs} is the volume of the internal pouch headspace, R is the gas universal constant, T is the storage temperature, m_{ss} is the dry mass of the packaged breadsticks, a_w^e is the external water activity, $y_1 = m_0 \cdot k \cdot C \cdot a_w^{int}(t)$, $y_2 = 1 - k \cdot a_w^{int}(t)$, $y_3 = 1 - k \cdot a_w^i(t) + C \cdot k \cdot a_w^{int}(t)$.

If the term related to the mass of water in the headspace of the internal pouch (i.e., $M_w \cdot \frac{p_w^0 \cdot V_{hs}}{R \cdot T}$) is neglected, the following relation is obtained:

$$\frac{da_w^{int}(t)}{dt} = \Theta \cdot \frac{\left(a_w^e - a_w^{int}(t)\right)}{\frac{m_0 \cdot k \cdot C \cdot \left(y_2 \cdot y_3\right) - y_1 \cdot \left[-k \cdot y_3 + y_2 \cdot (C \cdot k - k)\right]}{\left(y_2 \cdot y_3\right)^2}} \tag{7}$$

where: $\Theta = \frac{\xi \cdot p_w^0}{m_{ss}}$ expressed as $\frac{\frac{g\ H_2O}{g\ dm}}{day}$. It is worth noting that Θ is a constant. Equation (7) is an ordinary differential equation with $a_w^{int}(t)$ as unique unknown function. Solving this equation allows the description of the evolution of water activity within the primary package and, consequently, the estimation of the shelf life of the studied breadsticks.

A much simpler expression than Equation (7) can be obtained by further assuming a linear relationship between the water absorbed by the breadsticks and the water activity:

$$\frac{da_w^{int}(t)}{dt} = \beta \cdot \left(a_w^e - a_w^{int}(t)\right) \tag{8}$$

where: $\beta = \frac{\xi \cdot p_w^0}{m_{ss} \cdot \gamma}$ expressed as $\frac{1}{day}$, γ is the slope of the linear relationship used to describe the water sorption isotherm of the breadsticks. Equation (8) is a first-order kinetic equation with β as the kinetic constant, whose solution is given by:

$$a_w^{int}(t) = a_w^e + \left(a_w^0 - a_w^e\right) \cdot exp(-\beta \cdot t) \tag{9}$$

where: a_w^0 is the value of $a_w^{int}(t)$ at $t = 0$. Equation (9) can be rearranged as follow:

$$a_w^{int}(t) = a_w^e + \left(\frac{a_w^{max} - a_w^e \cdot [1 - exp(-\beta \cdot PSL)]}{exp(-\beta \cdot PSL)} - a_w^e\right) \cdot exp(-\beta \cdot t) \tag{10}$$

where: a_w^{max} is the threshold value of $a_w^{int}(t)$ beyond which the packaged breadsticks become unacceptable, PSL is the packaged food primary shelf life expressed in day. The advantage of using Equation (10) rather than Equation (9) is that, in the former, PSL is treated as a fitting parameter, allowing its uncertainty to be estimated from the fitting of experimental data.

3.2.3. Secondary shelf life

After the outer package is opened, only the internal pouch remains to protect the breadsticks. Since the phenomena involved are essentially the same, and under the same assumptions made previously, the following relation can be derived:

$$\frac{da_w^{int}(t)}{dt} = \Theta_A \cdot \frac{\left(a_w^e - a_w^{int}(t)\right)}{\frac{m_0 \cdot k \cdot C \cdot \left(y_2 \cdot y_3\right) - y_1 \cdot \left[-k \cdot y_3 + y_2 \cdot (C \cdot k - k)\right]}{\left(y_2 \cdot y_3\right)^2}} \tag{11}$$

where: $\Theta_A = \frac{A^{int} \cdot \frac{p_w^{int}}{\gamma^{int}} \cdot p_w^0}{m_{ss}}$ expressed as $\frac{\frac{g\ H_2O}{g\ dm}}{day}$.

Also in this case, a much simpler expression than Equation (11) can be obtained by further assuming a linear relationship between the water absorbed by the breadsticks and the water activity:

$$a_w^{int}(t) = a_w^e + \left(\frac{a_w^{max} - a_w^e \cdot [1 - exp(-\beta_A \cdot SSL)]}{exp(-\beta_A \cdot SSL)} - a_w^e\right) \cdot exp(-\beta_A \cdot t) \tag{12}$$

where: $\beta_A = \frac{A^{int} \cdot \frac{p_w^{int}}{\gamma^{int}} \cdot p_w^0}{m_{ss} \cdot \gamma}$ expressed as $\frac{1}{day}$, SSL is the secondary shelf life.

3.3. Validation

The models developed above to describe the water sorption isotherm and predict both primary and secondary shelf life were fitted to the experimental data. The quality of the fit was then used to evaluate the ability of the models, and the assumptions underlying their formulation, to accurately describe the mechanisms governing the deterioration of packaged breadsticks.

3.3.1. Water sorption isotherm

In Fig. 4 the experimental data of the water sorption isotherm of the investigated breadsticks are reported. The curve shown in the same figure was obtained by fitting Equation (1) to the experimental data. The values of the parameters obtained from the fitting are: $m_0 = 0.0683 \pm 0.0051\ \frac{g\ H_2O}{g\ dm}$, $k = 0.810 \pm 0.022$, and $C = 9.22 \pm 2.59$.

The goodness of fit was expressed by the mean of the relative deviation modulus ($\bar{E}\%$) (Buonocore et al., 2003):

$$\bar{E}\% = \frac{100}{N} \cdot \sum_{i=1}^{i=N} \frac{\left|M_i^{exp} - M_i^{pred}\right|}{M_i^{exp}} \tag{13}$$

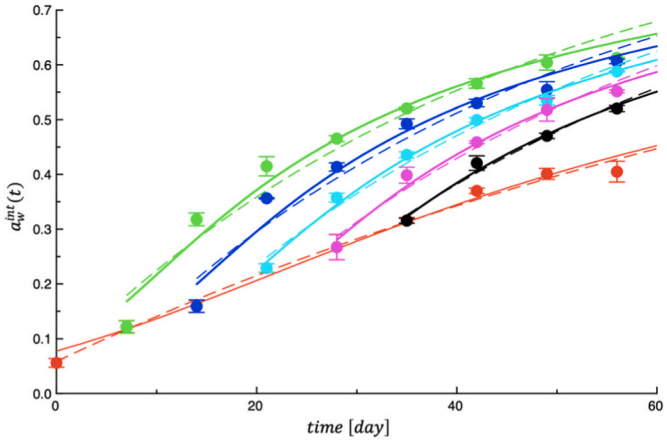

Fig. 5. ● Primary Shelf Life data. Time since the outer package was opened (TSO) ● TSO = 7 days, ● TSO = 14 days, ● TSO = 21 days, ● TSO = 28 days, ● TSO = 35 days; ——— Prediction of Equation (7); Prediction of Equation (11): ——— TSO = 7 days, ——— TSO = 14 days, ——— TSO = 21 days, ——— TSO = 28 days, ——— TSO = 35 days. – – – Prediction of Equation (10); Prediction of Equation (12): – – – TSO = 7 days, – – – TSO = 14 days, – – – TSO = 21 days, – – – TSO = 28 days, – – – TSO = 35 days.

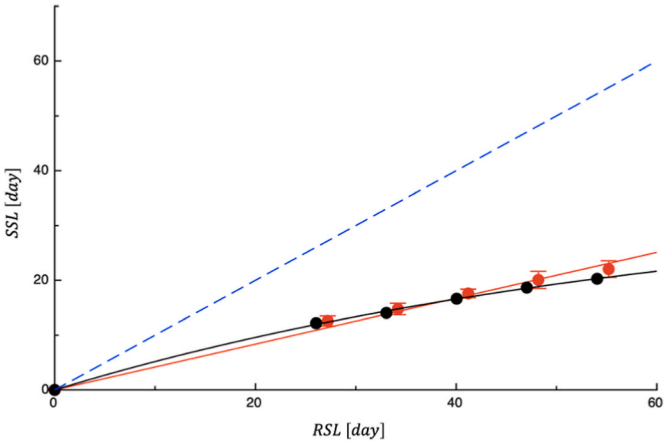

Fig. 6. ● data obtained using Equations (10) and (12), ● data obtained using Equations (7) and (11); ——— best fit of Equation (13); ——— this curve does not correspond to any model but is reported only to illustrate the trend of the data, – – – straight line with a slope equal to one.

where: N is the number of experimental data, M_i^{exp} is the experimental value, M_i^{pred} is the predicted value. With reference to the data reported in Fig. 5, an $\overline{E}\% = 5.58$ was obtained. This value can be considered satisfactory; therefore, it can be stated that the GAB model describes the water sorption isotherm of the studied breadsticks with sufficient accuracy. Collazos-Escobar et al. (2023) modelled the water adsorption isotherms of commercial Achira biscuits using GAB model together with several empirical models and machine-learning techniques. Their results demonstrated that both the GAB model and the alternative modelling approaches accurately described the combined effects of water activity and temperature on the equilibrium moisture content of the biscuits. Furthermore, the GAB model proved particularly useful in quantifying the effect of temperature on the adsorption properties, thus showing a lower hygroscopicity of the product at higher temperatures. Other findings in the literature demonstrate that GAB model facilitates parameter interpretation related to predictive model of shelf life, moisture migration, and quality degradation in low moisture food matrices. Comparing GAB parameters across studies is not straightforward, because of differences in sample composition and structure, drying and pre-treatment methods, data fitting procedures (Robertson and Lee, 2021). Dried products is a broad category that includes materials with different compositions, structures (amorphous *vs* crystalline), and porosities. These intrinsic differences strongly influence water sorption behaviour and, consequently, the estimated GAB parameters. It should also be noted that the experimental conditions used to determining sorption isotherms are often not standardized. Variations in temperature, relative humidity range, equilibration time, and use of adsorption or desorption isotherms may result in significant variations in the estimated model parameters. Since the GAB parameters are intrinsically temperature-dependent, even small differences in the experimental temperature may lead to appreciable variations in their estimated values. Consequently, direct comparison of GAB parameters reported in the literature, even for apparently similar dried products, should be undertaken with caution, only after carefully considering the experimental conditions and methodological approaches adopted in each study.

3.3.2. *Primary shelf life*

The first step in estimating the PSL and SSL of packaged breadsticks is to determine the water concentration threshold in the breadsticks (c_w^{max}) above which the product can be considered unacceptable, and

then calculate the corresponding water activity threshold.

In the present study a $c_w^{max} = 0.0915 \frac{g\ H_2O}{g\ dm}$, determined according to the method described in the Materials and Methods section, was found.

The value of a_w^{max} was obtained by inverting Equation (1) and expressing a_w^{max} as a function of c_w^{max}:

$$a_w^{max} = \frac{-\left(-k\cdot c_w^{max} + C\cdot k\cdot c_w^{max} - m_0\cdot k\cdot C\right) - \sqrt{\left(-k\cdot c_w^{max} + C\cdot k\cdot c_w^{max} - m_0\cdot k\cdot C\right)^2 - 4\cdot\left(k^2\cdot c_w^{max} - C\cdot k^2\cdot c_w^{max}\right)\cdot c_w^{max}}}{2\cdot\left(k^2\cdot c_w^{max} - C\cdot k^2\cdot c_w^{max}\right)} \quad (14)$$

The values of m_0, k, and C are those reported previously. In this specific case, a value of 0.4572 was obtained for a_w^{max}.

The external water activity (i.e., a_w^e), measured according to the method described in the Materials and Methods section, was 0.912 ± 0.005.

For PSL estimation based on Equation (7), Θ and a_w^0 are the only fitting parameters, whereas all other parameters appearing in the equation (i.e., a_w^e, m_0, k, and C) were fixed at the values previously reported. Equation (7) was numerically solved using the 4th-order Runge-Kutta formula (Press et al., 1989) and fitted to the experimental data.

Fig. 5 presents the fitting results, with the curve (solid line) representing the model (Equation (7)) and the dots indicating the experimental data. The fitting procedure yielded the following parameter values: $\Theta = 0.00164 \pm 8.65\cdot10^{-5} \frac{\frac{g\ H_2O}{g\ dm}}{day}$ and $a_w^0 = 0.0775 \pm 0.0086$; the mean of the relative deviation modulus ($\bar{E}$%) was found to be 7.28. Given the complexity of the phenomena involved and the assumptions made in deriving Equation (7), the obtained $\bar{E}$% value can be regarded as acceptable. Once the parameters of Equation (7) are estimated, the shelf life can be determined as the time at which $a_w^{int}(t) = a_w^{max}$. For this purpose, Equation (7) was evaluated over the time interval 0–60 days with a step size of 10^{-3} days, yielding a PSL = 61.0 days.

When Equation (10) was used to estimate primary shelf life, β and *PSL* were considered as the only fitting parameters, while all the other parameters appearing in the equation (i.e., a_w^{max}, a_w^e) were kept constant and equal to the values previously given. Fig. 6 shows the fitted curve (dashed line) obtained using Equation (10). The values of β and *SL* obtained from the fitting were $0.0101 \pm 0.000361 \frac{1}{day}$ and 62.2 ± 1.58 days, respectively, while the mean of the relative deviation modulus ($\bar{E}$%) was 3.73. In this case, the obtained $\bar{E}$% value is more than satisfactory and is lower than that obtained by fitting the same experimental data with Equation (7).

Since the two proposed models (i.e., Equation (7) and Equation (10)) differ only in the way the amount of water absorbed by the packaged breadsticks is estimated, it may initially appear surprising that Equation (10) provides a better fit to the experimental data shown in Fig. 6 than Equation (7). This observation seems counterintuitive because the sorption isotherm shown in Fig. 5 is clearly better described by the GAB model than by a linear relationship. The observed behaviour can be attributed to two main factors. First, in Equation (7) the parameters related to the water sorption isotherm (i.e., m_0, C, and k) were fixed, in Equation (10) the only isotherm-related parameter (i.e., γ) is included within one of the fitting parameters (i.e., β), thereby making Equation (10) slightly more flexible than the first one. Second, the water activity range investigated in the primary and secondary shelf-life tests is narrower than that used to determine the sorption isotherm; in the former case, a_w varies between 0.056 and 0.612, while in the latter it spans from 0.0992 to 0.9. The a_w range used for the shelf life tests was chosen based on the value of a_w^{max} (i.e., 0.4572). When focusing on the a_w range used in the shelf life tests, a linear approximation of the water sorption isotherm provides a description that is virtually indistinguishable from that of the GAB model. As shown in Fig. 5, the full isotherm is fitted using the GAB model, while a linear fit is applied to the data within the specified a_w range. For the reader's convenience, two dashed vertical lines indicate the limits of this range.

From the definitions of Θ, β, Θ_A, and β_A, the following relationship can be derived:

$$\frac{\Theta}{\beta} = \frac{\Theta_A}{\beta_A} = \gamma \quad (15)$$

Table 2 presents the values of γ, obtained from a linear fit of the experimental sorption isotherm data within the previously specified a_w range, together with the ratios $\frac{\Theta}{\beta}$ and $\frac{\Theta_A}{\beta_A}$. It is worth noting that the parameters Θ, β, Θ_A, and β_A were derived from the fitting of the kinetic data related to the primary and secondary shelf-life tests performed in this study. As shown by data in Table 2, the values of γ, $\frac{\Theta}{\beta}$ and $\frac{\Theta_A}{\beta_A}$ are very similar, with differences that are not statistically significant. This finding further confirms the hypothesis reported before on the reasons why both Equation (7) and Equation (10) provide an equal good description of the experimental data.

It should be emphasized that the accuracy of the models in describing the evolution of a_w^{int} during storage is critical for the determination of both PSL and SSL of packaged breadsticks. In this case, Equations (7) and (10) yielded primary shelf-life estimates of 61.0 and 62.2 ± 1.58 days, respectively. These values are in close agreement, as expected given the similarly low $\bar{E}$% values.

Comparison of the present findings with the available literature is inherently difficult because relatively few studies have addressed the prediction of primary shelf life in breadsticks or other low-moisture products based exclusively on moisture uptake as the quality-limiting mechanism. Most available research tends to focus on multiple quality indicators or different product categories (Corrigan et al., 2012; Calligaris et al., 2007) making direct comparisons difficult. For bakery products with a long shelf life, the peroxide value can be considered a representative indicator of quality deterioration. For example, Calligaris et al. (2008) validated the predictive protocol previously proposed by

Table 2

Values of γ together with the ratios $\frac{\Theta}{\beta}$ and $\frac{\Theta_A}{\beta_A}$ at different TSO. Data are reported as means ± standard deviation (std); data with different superscript letter are statistically different ($p < 0.05$).

Parameter	Mean ± std
γ	0.150 ± 0.00989^{a}
$\frac{\Theta}{\beta}$	0.162 ± 0.0104^{a}
$\frac{\Theta_A}{\beta_A}$ (TSO = 7 day)	$0.173 \pm 2.18\cdot10^{-2\ a}$
$\frac{\Theta_A}{\beta_A}$ (TSO = 14 day)	$0.170 \pm 2.50\cdot10^{-2\ a}$
$\frac{\Theta_A}{\beta_A}$ (TSO = 21 day)	$0.167 \pm 1.27\cdot10^{-2\ a}$
$\frac{\Theta_A}{\beta_A}$ (TSO = 28 day)	$0.166 \pm 2.08\cdot10^{-2\ a}$
$\frac{\Theta_A}{\beta_A}$ (TSO = 35 day)	$0.163 \pm 2.19\cdot10^{-2\ a}$

Table 3
Values of the parameters obtained from the fitting, together with the $\overline{E}$% values, at various times since the outer package was opened (TSO). Data are reported as means ± standard deviation (std); data in the same column with different superscript letter are statistically different ($p < 0.05$).

TSO [day]	Equation (11)				Equation (12)		
	$\Theta_A \left[\frac{g\,H_2O}{\frac{g\,dm}{day}}\right]$	a_w^0	*SSL* [*day*]	$\overline{E}$%	$\beta_A \left[\frac{1}{day}\right]$	*SSL* [*day*]	$\overline{E}$%
7	0.00375 ± 0.000311^{a}	0.168 ± 0.0222^{a}	20.3	8.11	0.0217 ± 0.00205^{a}	22.0 ± 1.51^{a}	10.6
14	0.00369 ± 0.000362^{a}	$0.199 \pm 0.0243^{a,b}$	18.7	7.15	0.0216 ± 0.00236^{a}	$20.07 \pm 1.57^{a,b}$	9.22
21	0.00358 ± 0.000152^{a}	$0.240 \pm 0.00918^{b,c}$	16.6	2.13	0.0215 ± 0.00135^{a}	$17.6 \pm 0.788^{b,c}$	3.80
28	0.00358 ± 0.000271^{a}	$0.280 \pm 0.0136^{c,d}$	14.1	2.56	0.0215 ± 0.00214^{a}	$14.8 \pm 1.05^{c,d}$	3.88
35	0.00329 ± 0.000276^{a}	0.323 ± 0.0109^{d}	12.2	1.82	0.0202 ± 0.00211^{a}	12.57 ± 0.921^{d}	2.27

Calligaris et al. (2007), demonstrating its applicability for estimating the shelf life of dry bakery products with a commercial shelf life exceeding 100 days.

They evaluated peroxide value changes related to the sensory acceptance limit and found predictive equations able to describe the temperature dependence of peroxide formation. In addition, the variability in packaging and storage conditions across different studies further complicates any direct comparison, as these factors can significantly influence the outcomes. A few years ago, the study conducted by Alamprese et al. (2017) investigated strategies to extend the shelf life of breadsticks by using rosemary extract, modified atmosphere packaging, and a combination of both approaches. Although their work provides useful insights into shelf life prediction for bakery products, it does not specifically address water uptake as the sole quality-limiting factor. Instead, the authors identified lipid oxidation as the main mechanism responsible for the quality deterioration of whole-wheat breadsticks, further highlighting the limited availability of studies that can be directly compared with the present work extension techniques. These authors confirmed that quality decay of whole-wheat breadsticks was mainly associated to lipid oxidation. The kinetic study of oxidation development and the consumer sensory acceptance determined by the survival analysis demonstrated that the rosemary extract addition yields a 42% shelf life extension, higher than that observed using nitrogen in the package (24–29%). The combination of the formulation and packaging strategies gave the best result (83% shelf life extension at 25 °C).

3.3.3. Secondary shelf life

Fig. 5 presents a_w^{int} plotted as a function of storage time after the opening of the primary package. As expected, the increase in water activity is faster after the opening of the primary package than when it remains intact. This holds for each value of the time since the outer package was opened (TSO). The curves (solid line) in the figure represent the best fit of Equation (11) to the experimental data. The fitted parameter values are reported in Table 3, along with the corresponding $\overline{E}$% values. As indicated by the $\overline{E}$% values reported in the table, Equation (11) provides a satisfactory description of the experimental data. It is also worth noting that, in accordance with its definition, Θ_A is independent by TSO and it is consistently higher than Θ. Although slight variations in Θ_A are observed as TSO changes, these differences are not statistically significant. The curves (dashed line) shown in Fig. 6 were obtained by fitting Equation (12) to the experimental data (i.e., a_w^{int} vs. storage time). The values of the parameters obtained from the fitting are also reported in Table 3, together with the $\overline{E}$% values. As before, the E% values suggest that the proposed model describes the experimental data with sufficient accuracy. It should be noted that the β_A values are practically independent by the TSO value and consistently lower than β, as expected given the definition of β_A. As previously noted for θ_A, slight variations in β_A values were observed with changing TSO, but these differences are not statistically significant.

Similarly to PSL, the two proposed models (i.e., Equations (11) and (12)) provide an equally good description of the experimental data, given the small differences in their respective $\overline{E}$% values. The same observations previously made for PSL hold for SSL as well.

Direct comparison of the present results on secondary shelf life with those reported in the literature is particularly difficult. Studies specifically addressing secondary shelf life of dry bakery products remains scarce, and the available investigations generally define product deterioration after package opening using different quality criteria. Furthermore, most of these studies consider multiple deterioration mechanisms, whereas the present work focuses exclusively on moisture uptake as the quality-limiting factor, making meaningful comparisons inherently limited. For example, Anese et al. (2006) assessed the secondary shelf life of ground roasted coffee. The changes of some chemical and physicochemical indexes of coffee staling were studied, and sensory analysis was carried out to determine the end point of coffee acceptability. Then, sensory and instrumental results were used to develop a mathematical model allowing to simply and quickly calculate the secondary shelf life of coffee on the basis of its a_w value at a given temperature. Moreover, differences in packaging systems, package-opening conditions, and post-opening storage environments (such as relative humidity and temperature) further increase the variability among studies, making direct comparison of the reported results even more difficult. The approach generally adopted by researchers is to assess the SSL of food, and its dependence on packaging systems or storage conditions after the package opening (Del Nobile and Conte, 2023). As previously stated, the proposed approach aims to quantify the influence of the product deterioration state at the time of package opening on SSL. In other words, SSL is related to the extent to which the reactions responsible for quality loss have progressed before the package is opened.

3.4. Secondary shelf life vs residual shelf life

Fig. 6 presents SSL as a function of RSL. The SSL values correspond to those reported in Table 3, while the RSL values were calculated according to the definition previously given and using the PSL values reported earlier for the two proposed models (i.e., Equation (7) and Equation (10)). The same figure also includes a straight line with unit slope (dashed line). For each RSL value, the difference between this line and the SSL, estimated according to the previously described procedure, represents the loss of shelf life resulting from the primary package opening. Since opening the primary package accelerates the quality decay kinetics of the packaged food, the SSL values can only approach, but never reach, the 45° line. The smaller the impact of the primary packaging on shelf life, the closer the SSL values lie to the 45° line. As expected, a decrease in RSL is accompanied by a decrease in SSL. As shown in the figure, the two proposed models produce very similar results, especially at low RSL values, while the differences become more pronounced as RSL increases. This is in full agreement with the findings previously reported.

For the data obtained using Equations (7) and (11), the curve shown in Fig. 6 is intended only as a visual guide to the data trend and does not correspond to any mathematical model or fitting function. Under the

first-order quality decay kinetics, SSL can be shown to increase linearly with RSL using an approach analogue to that proposed by Lacivita et al. (2023). Therefore, for the data obtained using Equations (10) and (12), the following relationship applies:

$$SSL = \frac{\beta}{\beta_A} \cdot RSL \tag{13}$$

Fitting the data in Fig. 6 with a straight line passing through the origin yields a slope of 0.418 ± 0.008. Using the data obtained previously, the ratio $\frac{\beta}{\beta_A}$ is equal to 0.475 ± 0.05. The difference between the value obtained from the best fit of the data and that calculated using the data obtained previously is small and not statistically significant. These results further support the validity of the assumptions underlying the derivation of Equations (10) and (12).

From the previously given definitions of β and β_A, the following relationship can be derived:

$$\frac{\beta}{\beta_A} = \frac{1}{1 + \frac{A^{int} \cdot \frac{p_w^{int}}{r^{int}}}{A^{est} \cdot \frac{p_w^{est}}{r^{est}}}} \tag{14}$$

As indicated by Equation (14), the ratio $\frac{\beta}{\beta_A}$ tends to 1 when $A^{est} \cdot \frac{p_w^{est}}{r^{est}}$ is much larger than $A^{int} \cdot \frac{p_w^{int}}{r^{int}}$, that is, when the water vapor flux through the outer film greatly exceeds that through the inner packaging. This is in full agreement with the previous discussion. Indeed, the higher the flux through the outer film, the less its opening affects the SSL, which tends to converge to the same value as RSL.

To the best of our knowledge, no previous studies have explicitly investigated how the timing of package opening influences the subsequent secondary shelf life of breadsticks or other similar dry bakery products. This lack of information makes it difficult to place the present findings within an established scientific framework. In this context, the proposed approach provides novel insights by demonstrating that secondary shelf life is strongly dependent on the product deterioration state at the time of the package opening, which reflects its residual primary shelf life. By quantitively describing this relationship, the present study helps fill an important gap in the literature and offers a more comprehensive framework for understanding and predicting shelf life evolution in dry bakery products.

4. Conclusions

The present study investigated the relationship between secondary shelf life (SSL) and residual shelf life (RSL) in packaged breadsticks. Since the evolution of water activity inside the package ($a_w^{int}(t)$), plays a key role in determining product stability, particular attention was devoted to its mathematical description. Two alternative modelling approaches were developed. The first combines the package mass balance with the GAB sorption isotherm, resulting in a differential equation that requires numerical solution. The second adopts a linear approximation of the sorption isotherm, leading to an explicit analytical expression for $a_w^{int}(t)$. Although the GAB model provides a more rigorous description of the entire sorption isotherm, both approaches were found to reproduce the experimental data with comparable accuracy. This result can be explained by the limited range of water activity explored during the shelf-life tests. Because product acceptability is lost at relatively low water activity values ($a_w^{max} = 0.4572$), only the initial portion of the sorption isotherm is relevant to the analysis. Within this region, the GAB and linear models provide nearly identical predictions, leading to equivalent estimates of water activity evolution and shelf life. Considering that the simpler model achieves the same predictive performance while avoiding numerical integration, it represents the most practical solution for describing the behaviour of the system. Furthermore, both approaches predict essentially the same relationship between SSL and RSL. In the case of the linear model, this relationship is accurately represented by a straight line passing through the origin, indicating a direct proportionality between the two quantities. Overall, the results demonstrate that a simple analytical framework can successfully predict the secondary shelf life of packaged breadsticks from their residual shelf life, providing a practical tool for shelf-life assessment and package management.

One limitation of the proposed model is that it does not account for the possible dependence of film water vapor permeability on the water activity conditions on either side of the packaging material. However, this limitation is expected to have only a minor impact on the results. Indeed, packaging systems intended for low-moisture products such as breadsticks generally employ high-barrier materials whose permeability is only weakly affected by the surrounding humidity conditions. Consequently, the assumption of constant permeability is considered reasonable for the packaging materials and storage conditions investigated in this study. Another limitation is that the kinetic parameters appearing in the model were assumed to be constant under the experimental conditions considered. Although these parameters are inherently temperature-dependent, the objective of the present study was not to investigate their temperature dependence, but rather to validate a modelling framework capable of describing both the primary and secondary shelf life of packaged breadsticks. The incorporation of temperature-dependent kinetic parameters, as well as the evaluation of their variation with storage conditions, will be addressed in future studies. Future developments may therefore include both the incorporation of water-activity-dependent permeability and the explicit description of the temperature dependence of the model parameters, thereby extending the applicability of the proposed approach to a wider range of packaging systems and storage conditions.

Ethical declaration

The study was approved by the Ethics Committee "COMITATO ETICO PER LA RICERCA DELL'UNIVERSITÀ DI MODENA E REGGIO EMILIA (CEAR)" (approval date: 09/01/2025; Protocol No. 4569). All participants provided informed consent prior to participation. All members in the sensory analysis participated voluntarily after signing an informed consent form, which included a description of the study and any potential risks. Furthermore, all data were kept confidential and handled in accordance with privacy regulations.

CRediT authorship contribution statement

Emanuela Lo Faro: Investigation, Methodology, Writing – original draft. **Francesca Masino:** Investigation, Methodology, Writing – original draft. **Patrizia Fava:** Conceptualization, Supervision, Writing – original draft. **Matteo Alessandro Del Nobile:** Conceptualization, Methodology, Validation, Writing – original draft. **Amalia Conte:** Conceptualization, Supervision, Writing – review & editing.

Declaration of competing interest

The authors declare that they have no known competing financial interests or personal relationships that could have appeared to influence the work reported in this paper.

Data availability

Data will be made available on request.

References

Afsharnia, F., 2023. Optimization of in vitro and in vivo antifungal effects of trehalose coating included *Artemisia sieberi* essential oil on mulberry (*Morus alba* var. *nigra*) fruits using the hybrid RSM-GRA method. Food Sci. Biotechnol. 32, 921–935.

Al-Muhtaseb, A.H., McMinn, W.A.M., Magee, T.R.A., 2002. Moisture sorption isotherm characteristics of food products: a review. Food Bioprod. Process. 80 (2), 118–128.

Alamprese, C., Cappa, C., Ratti, S., Limbo, S., Signorelli, M., Fessas, D., Lucisano, M., 2017. Shelf life extension of whole-wheat breadsticks: formulation and packaging strategies. Food Chem. 230, 532–539.
Anese, M., Manzocco, L., Nicoli, M.C., 2006. Modeling the secondary shelf-life of ground roasted coffee. J. Agric. Food Chem. 54, 5571–5576.
ASTM, 2024. E96/96M-24a Standard Test Methods for Gravimetric Determination of Water Vapor Transmission Rate of Materials. ASTM International, West Conshohocken, PA, USA.
Barbosa-Cánovas, G.V., Fontana, A.J., Schmidt, S., Labuza, T.P., 2007. Water Activity in Foods: Fundamentals and Applications. IFT Press-Blackwell Publishing, Oxford, UK.
Bianchi, A., Taglieri, I., Macaluso, M., Sanmartin, C., Zinnai, A., Venturi, F., 2023. Effect of different packaging strategies on the secondary Shelf life of young and structured red wine. Foods 16; 12 (14), 2719. https://doi.org/10.3390/foods12142719. PMID: 37509811; PMCID: PMC10379816.
Bianchi, A., Venturi, F., Palermo, C., Taglieri, I., Angelini, L.G., Tavarini, S., Sanmartin, C., 2024. Primary and secondary shelf-life of bread as a function of formulation and MAP conditions: focus on physical-chemical and sensory markers. Food Pack. Shelf Life 41, 101241.
Bianchi, F., Lomuscio, E., Rizzi, C., Simonato, B., 2021. Predicted Shelf-life, thermodynamic study and antioxidant capacity of breadsticks fortified with grape pomace powders. Foods 10, 2815. https://doi.org/10.3390/foods10112815.
Buonocore, G.G., Del Nobile, M.A., Di Martino, C., Gambacorta, G., La Notte, E., Nicolais, L., 2003. Modeling the water transport properties of casein-based edible coating. J. Food Eng. 60, 99–106.
Calligaris, S., Manzocco, L., Kravina, G., Nicoli, C.M., 2007. Shelf-life modeling of bakery products by using oxidation indices. J. Agric. Food Chem. 55, 2004–2009.
Calligaris, S., Pieve, S.D., Kravina, G., Manzocco, L., Nicoli, C.M., 2008. Shelf life prediction of bread sticks using oxidation indices: a validation study. J. Food Sci. 73, E51–E56.
Cesa, S., Casadei, M.A., Cerreto, F., Paolicelli, P., 2015. Infant milk formulas: effect of storage conditions on the stability of powdered products towards autoxidation. Foods 4 (3), 487–500. https://doi.org/10.3390/foods4030487, 22.
Chen, P., Chau, C., 2026. Label-Centric review of food labeling interventions for reducing food waste: a motivation–opportunity–ability framework-based perspective. Sustain. 18, 3725. https://doi.org/10.3390/su18083725.
Coffigniez, F., Matar, C., Gaucel, S., Gontard, N., Guilbert, S., Guillard, V., 2021. The use of modeling tools to better evaluate the packaging benefice on our environment. Front. Sustain. Food Syst. 5, 634038. https://doi.org/10.3389/fsufs.2021.634038.
Collazos-Escobar, G.A., Gutierrez-Guzman, N., Vaquiro-Herrera, H.A., Bon, J., Carcel, J. A., García-Perez, J.V., 2023. Model-based investigation of water adsorption in Achira (Canna edulis K.) biscuits. LWT Food Sci. Technol. 189, 115472.
Corrigan, V., Hedderley, D., Harvey, W., 2012. Modeling the shelf life of fruit filled snack bars using survival analysis and sensory profiling techniques. J. Sensory Stud. 27, 403–416.
Cui, F., Zheng, S., Wang, D., Tan, X., Li, Q., Li, J., Li, T., 2023. Recent advances in shelf life prediction models for monitoring food quality. Compr. Rev. Food Sci. Food Saf. 22 (2), 1257–1284.
Del Nobile, M.A., Conte, A., 2023. Secondary Shelf life of foods: state of the art and future perspective. Food Eng. Reviews 15, 748–762.
Giuffrè, A.M., Caracciolo, M., Zappia, C., Capocasale, M., Poiana, M., 2023. Breadsticks flavoured with olives and onions: One-Year Shelf life. Foods 12, 1798. https://doi.org/10.3390/foods12091798.
Jia, H., Li, Y., Zhao, T., Li, Z., Yang, X., Zhang, W., Zhao, Q., Jiang, Y., 2025. Quality and flavor evolution of infant formula during simulated secondary shelf-life storage: focus on volatile compounds at different storage temperatures. Food Res. Int. 221 (Pt 3), 117428.
Lacivita, V., Lordi, A., Conte, A., Del Nobile, M.A., 2023. Study on the influence of visible molds on primary and secondary shelf life of pasteurized gnocchi. Food Biosci. 56, 103131.
Lee, D.S., Robertson, G.L., 2021. Interactive influence of decision criteria, packaging film, storage temperature and humidity on shelf life of packaged dried vegetables. Food Pack. Shelf Life 28, 100674.
Li, Y., Li, R., Hu, X., Liu, J., Liu, G., Gao, L., Zhang, Y., Wang, H., Zhu, B., 2024. Changes of the volatile compounds and odors in one-stage and three-stage infant formulas during their secondary shelf-life. Curr. Res. Food Sci. 8, 100693.
Lo Faro, E., Menozzi, C., Licciardello, F., Fava, P., 2021. Improvement of paper resistance against moisture and oil by coating with poly(-3-hydroxybutyrate-co-3-hydroxyvalerate)(PHBV) and Polycaprolactone (PCL). Appl. Sci. 11 (17), 8058.
Martinelli, E., De Canio, F., Sarti, E., 2025. Reducing Food waste through the secondary shelf life indication: exploring consumer motives and behaviors. In: Sinergie-SIMA 2025 Management Conference. Conference Proceedings. Long Papers. FONDAZIONE CUEIM, pp. 427–441. https://doi.org/10.7433/SRECP.LP.2025.01.
McMinn, W.A.M., McKee, D.J., Magee, T.R.A., 2007. Moisture adsorption behaviour of oatmeal biscuit and oat flakes. J. Food Eng. 79 (2), 481–493.
Mora, R.L., Vanare, S.P., Pegg, R.B., 2025. Mechanisms, causes, and solutions: a comprehensive review of lipid oxidation in low-moisture packaged snacks. Eur. J. Lipid Sci. Technol. 127, e70044.
Nicoli, M.C., Calligaris, S., 2018. Secondary shelf life: an underestimated issue. Food Eng. Rev. 10, 57–65.
Nicosia, C., Fava, P., Pulvirenti, A., Licciardello, F., 2022. Secondary shelf life assessment of UHT milk and its potential for food waste reduction. Food Pack. Shelf Life 33, 100880.
Panel, E.B., Koutsoumanis, K., Allende, A., Alvarez-Ordonez, A., Bolton, D., Bover-Cid, S., Chemaly, M., Davies, R., De Cesare, A., Herman, L., et al., 2020. Guidance on date marking and related food information: part 1 (date marking). EFSA J. 18, 74.
Piergiovanni, L., Limbo, S., 2019. Food shelf-life models. In: Accorsi, R., Manzini, R. (Eds.), Sustainable Food Supply Chains. Academic Press, pp. 49–60.
Press, Flannery, Teukolsky, Vetterling, Press, W.H., Flannery, B.P., Teukolsky, S.A., Vetterling, W.T., 1989. Numerical Recipes in Pascal. Univ. Press, Cambridge, p. 602.
Robertson, G.L., Lee, D.S., 2021. Comparison of linear and GAB isotherms for estimating the shelf life of low moisture foods packaged in plastic films. J. Food Eng. 291.
Salimbahrami, S.N., Ghorbani-HasanSaraei, A., Tahermansouri, H., Shahidi, S.A., 2023. Synthesis, optimization via response surface methodology, and structural properties of carboxymethylcellulose/curcumin/graphene oxide biocomposite films/coatings for the shelf-life extension of shrimp. Int. J. Biol. Macromol. 253, 126724.
Sordini, B., Esposto, S., Bonucci, A., Dottori, I., Daidone, L., Urbani, S., Veneziani, G., Selvaggini, R., Servili, M., Nucciarelli, D., et al., 2025. Role of a natural antioxidant in the secondary Shelf life of ready-to-use meat pâté. Proceedings 119, 10. https://doi.org/10.3390/proceedings2025119010.
Sordini, B., Urbani, S., Esposto, S., Selvaggini, R., Daidone, L., Veneziani, G., Servili, M., Taticchi, A., 2024. Evaluation of the effect of an olive phenolic extract on the secondary Shelf life of a fresh pesto. Antioxidants 13, 128. https://doi.org/10.3390/antiox13010128.
Türksever, C., Koç, B., Kizilirmak Esmer, O., 2025. Sustainable alternatives in multilayer packaging: storage stability of pudding powder under accelerated storage conditions. Foods 14 (22), 3806.
WRAP, 2023. Behaviour Change Intervention: Day on the Date Label. WRAP, Banbury, UK.
Zardetto, S., Fregonese, M., Pasini, G., 2022. Effects of modified atmospheric packaging configuration on spoilage mould growth in damaged packages of fresh pasta. J. Food Eng. 314, 110760. https://doi.org/10.1016/j.jfoodeng.2021.110760.